Detection of pulmonary embolism with free-breathing dynamic contrast-enhanced MR imaging

Michael Ingrisch[1†], Daniel Maxien[2†], Felix G. Meinel[2], Maximilian F. Reiser[2], Konstantin Nikolaou[2,3], Olaf Dietrich[1]

[1]Josef-Lissner-Laboratory for Biomedical Imaging, Institute for Clinical Radiology, Ludwig-Maximilians-University Hospital Munich, Marchioninistr. 15, 81377 Munich, Germany

[2]Institute for Clinical Radiology, Ludwig-Maximilians-University Hospital Munich, Marchioninistr. 15, 81377 Munich, Germany

[3]Department of Diagnostic and Interventional Radiology, Eberhard-Karls-University, Hoppe-Seyler-Str. 3, 72076 Tübingen, Germany

[†]M.I. and D.M contributed equally

This work has been supported by grants of the Deutsche Forschungsgemeinschaft (DFG grants DI1413/2-2 and NI 707/1-3).

Abstract

Purpose: **To evaluate the use of dynamic contrast-enhanced (DCE) MRI during free breathing for the detection of acute pulmonary embolism (PE).**

Materials and Methods: **Eighteen subjects underwent free-breathing DCE MRI at 1.5T, 8 of which were patients with acute PE, as confirmed by routine CT pulmonary angiography (CTPA). The remaining ten subjects were healthy volunteers with no history or signs of pulmonary disease.**

From all DCE MRI data, maps of relative signal enhancement were calculated and assessed for the presence or absence of perfusion defects in each lung by two readers. Inter-reader variability, sensitivity and specificity of free-breathing DCE MRI for the detection of PE were calculated using CTPA as gold standard.

Results: **Of the 16 patient's lungs , 15 were affected from acute PE, according to CTPA. In patients and volunteers, DCE MRI sensitivity was 93% and 87% for reader 1 and 2, with specificities of 95% and 90%, respectively. Inter-reader agreement was substantial, with $\kappa = 0.77$ $(95\%\ CI, 0.44 - 1.0)$.**

Conclusion: **Free-breathing DCE MRI may have potential use for the assessment of PE, and does not require patient cooperation in breath-holding.**

Keywords

Dynamic contrast-enhanced MRI; Lung; pulmonary embolism; perfusion

Corresponding author:

Michael Ingrisch
Josef-Lissner-Laboratory for Biomedical Imaging
Institute for Clinical Radiology
Ludwig-Maximilians-University Hospital Munich
Marchioninistr. 15, 81377 Munich, Germany

michael.ingrisch@med.lmu.de
Phone +49 89 4400 74624
Fax +49 89 4400 74624

Introduction

Pulmonary embolism (PE) is a common condition responsible for substantial morbidity and mortality (1, 2). Since clinical symptoms and laboratory findings may be non-specific, imaging tests are often needed to diagnose PE and thus enable appropriate treatment.

Imaging of pulmonary embolism can focus on visualization of either the cause or the effects of PE. The former strategy aims at directly displaying the blood clots that occlude the pulmonary arteries, whereas the latter strategy displays the perfusion defects that are caused by these blood clots. The standard technique for the direct visualization of a pulmonary embolus or thrombus is contrast-enhanced computed tomography pulmonary angiography (CTPA), where the blood clots appear hypodense relative to the surrounding arterial blood, opacified with contrast agent (3–6). Direct visualization is also possible in magnetic resonance imaging: Magnetization-prepared sequences display blood clots with a bright signal (7, 8); steady state free precession gradient echo sequences, on the other hand, display flowing blood with bright signal, so that blood clots appear hypointense (9).

Functional imaging techniques, on the other hand, visualize the perfusion deficits that are caused by occlusions in the pulmonary arteries. Usually, this is achieved by intravenous administration of a suitable radio tracer or contrast agent before image acquisition. The differences in signal intensity between perfused and non-perfused lung regions allow for an assessment of the affected lung regions. For this purpose, lung scintigraphy has long been used for imaging of patients with suspected PE (8). More recently, dual-energy CT has been proposed for this purpose (10–13). Both methods have the drawback that the patient is exposed to ionizing radiation. A recently proposed method, Fourier decomposition MRI, allows imaging of pulmonary ventilation and perfusion during free breathing without the application of contrast agent, and has been shown to be useful for the diagnosis of chronic PE without the use of ionizing radiation (14).

Dynamic contrast-enhanced (DCE) MRI can also be used for the detection of pulmonary embolism (15), with the additional benefit that the acquisition is not limited to a single or a few time frames like in CT, but can be performed continuously. From DCE MRI data, parameters like the pulmonary blood flow and blood volume can be calculated quantitatively (16, 17), even when the measurement is performed not under breath hold, but during free breathing (18, 19). For the mere diagnosis of pulmonary embolism, however, the evaluation of a single time frame with strong perfusion weighting such as the time point of maximal pulmonary enhancement may be sufficient. This time point can be selected retrospectively, so that the timing is much less critical than in contrast-enhanced CT. Since DCE MRI is usually performed with a temporal resolution in the order of seconds, breathing-related motion within each single time frame is minimized. Therefore, it may even be possible to reliably assess pulmonary embolism on data acquired during free breathing. Additionally, a dynamic acquisition allows for suppression of the background signal by converting the signal intensity to contrast agent concentration, e.g., by calculation of signal enhancement (20).

The aim of this study was to prospectively assess the feasibility and potential value of free-breathing pulmonary DCE MRI for the diagnosis of pulmonary embolism.

Methods

Patients and Volunteers

In this institutional review-board approved study, 18 subjects underwent a DCE MRI examination during free breathing. Ten of these subjects were healthy volunteers with no history or signs of pulmonary disease. 8 of the subjects were patients who had undergone a clinically indicated CTPA which confirmed acute PE. Written informed consent was obtained from patients and volunteers after the nature of the procedures had been fully explained. The MRI examination was performed within 5 days (mean 3 days, range 1-5 days) after the CTPA and included a DCE measurement. Exclusion criteria for MRI were claustrophobia, pacemakers or other metal implants not suitable for MRI, known allergy to MRI contrast agents and renal impairment (estimated glomerular filtration rate <60 mL/min).

Imaging

All MR examinations were performed on a 1.5T MRI scanner (Magnetom Aera, Siemens Healthcare, Erlangen, Germany), using a 16-channel spine array coil and an 18-channel body matrix coil. For the dynamic acquisition, a 3D spoiled gradient echo sequence (time-resolved angiography with stochastic trajectories, TWIST; TE/TR=0.9 ms/2.0 ms) accelerated with view sharing and parallel imaging was used as described previously (18, 19). Detailed sequence parameters are given in Table 1. After intravenous injection of a body-weight adapted dose of contrast agent (0.1 mmol/kg bodyweight of gadobutrol, Gadovist, Bayer Healthcare, Berlin, Germany) with a flow rate of 3mL/s, followed by a saline flush of 25mL, 110 coronal volumes (phase encoding direction: left-right) were recorded with a temporal resolution of 1.3 seconds per volume, amounting to a total measurement time of 146 seconds. Subjects were instructed to breathe shallowly throughout the entire examination.

Table 1: DCE MRI acquisition parameters

TE/TR	0.9 ms/2.0 ms
Matrix size	128×128×36
Spatial resolution	3×3×4 mm³
Temporal resolution	1.3 s
Flip angle	15°
Bandwidth	1115 Hz/pixel
Parallel Imaging	GRAPPA, *R*=2, 24 reference lines
Total acquisition time	146 s
Acquired volumes	110

CTPA examinations were performed on a dual-source CT scanner (Somatom Definition Flash; Siemens Healthcare, Forchheim, Germany). An 85 mL bolus of contrast medium (iopromide, Ultravist 370; Bayer Healthcare, Berlin, Germany) was administered via an antecubital vein at a flow rate of 5 mL/s, followed by 50 mL of saline injected at the same flow rate. Scans were automatically started 7 seconds after a pre-specified attenuation threshold of 100 Hounsfield unit (HU) was reached in a region of interest placed in the main pulmonary artery. Images of the entire thorax were acquired during breath-hold in inspiration. To minimize potential streak artifacts from concentrated contrast material in the superior vena cava, images were acquired in caudocranial direction. Collimation was set to 32 × 0.6 mm, a pitch factor of 0.5 and a rotation time of 0.28 seconds were used. Transverse and coronal image series were reconstructed at a slice thickness of 1.5 mm with 1 mm increment using a medium soft vascular reconstruction kernel.

Image Analysis

Post-processing and visualization of the DCE MRI data were performed in a dedicated postprocessing software (Slicer 4.3, (21)) with a custom-written plug-in. Briefly, a map of the baseline signal S_0 was calculated by averaging over all time points before the arrival of contrast agent. The relative signal enhancement $RSE(t) = \frac{S(t)-S_0}{S_0}$ was calculated for each voxel, resulting in a 4D dataset of pulmonary enhancement.

In the resulting maps of relative signal enhancement, the presence or absence of perfusion defects in each lung at the time point of maximal pulmonary enhancement was evaluated. (All areas with decreased perfusion visible on the maps of relative signal enhancement were counted as perfusion defects.) To calculate inter-reader variability, this reading was performed by two radiologists with 6 and 4 years of experience in pulmonary imaging (DM, FM). The order of patients and volunteers was randomized before reading; readers were blinded to each other's results, to the origin of the dataset (patient or volunteer) and to the CTPA results, if available.

In the CTPA, the presence or absence of obstructing blood clots in the pulmonary arteries in each lung was evaluated by reader 1 (DM, 6 years of experience in thoracic CT).

Statistical Analysis

Statistical analysis was done in R (22). Inter-reader agreement was evaluated using Cohen's kappa. Sensitivity, specificity, positive and negative predictive values of DCE MRI relative signal enhancement were calculated against the gold standard CTPA. The agreement between CTPA and DCE MRI was assessed using Fisher's exact test.

Results

All volunteer and patient measurements were completed without complications. Patient data is shown in Table 2.

Compared to the unprocessed raw data, the calculation of the relative signal enhancement yielded images with suppressed background signal and strong enhancement of perfused pulmonary parenchyma, in particular during peak pulmonary enhancement (Fig. 1). Figure 2 shows CTPA images with the thrombi corresponding to the perfusion defects in Fig. 1. The difference in relative signal enhancement between perfused and non-perfused regions is maximal during the bolus passage, whereas in later phases, the relative signal enhancement in these regions is similar (Fig. 3). During peak enhancement, perfusion defects are clearly visible (Figs. 1 and 4).

Table 2: Patient data

Subject ID	Age	Sex	Time between CT and MRI in days
2	36	f	4
3	68	f	5
6	41	f	3
7	44	m	2
10	81	f	3
14	44	m	1
15	50	f	2
17	70	m	2

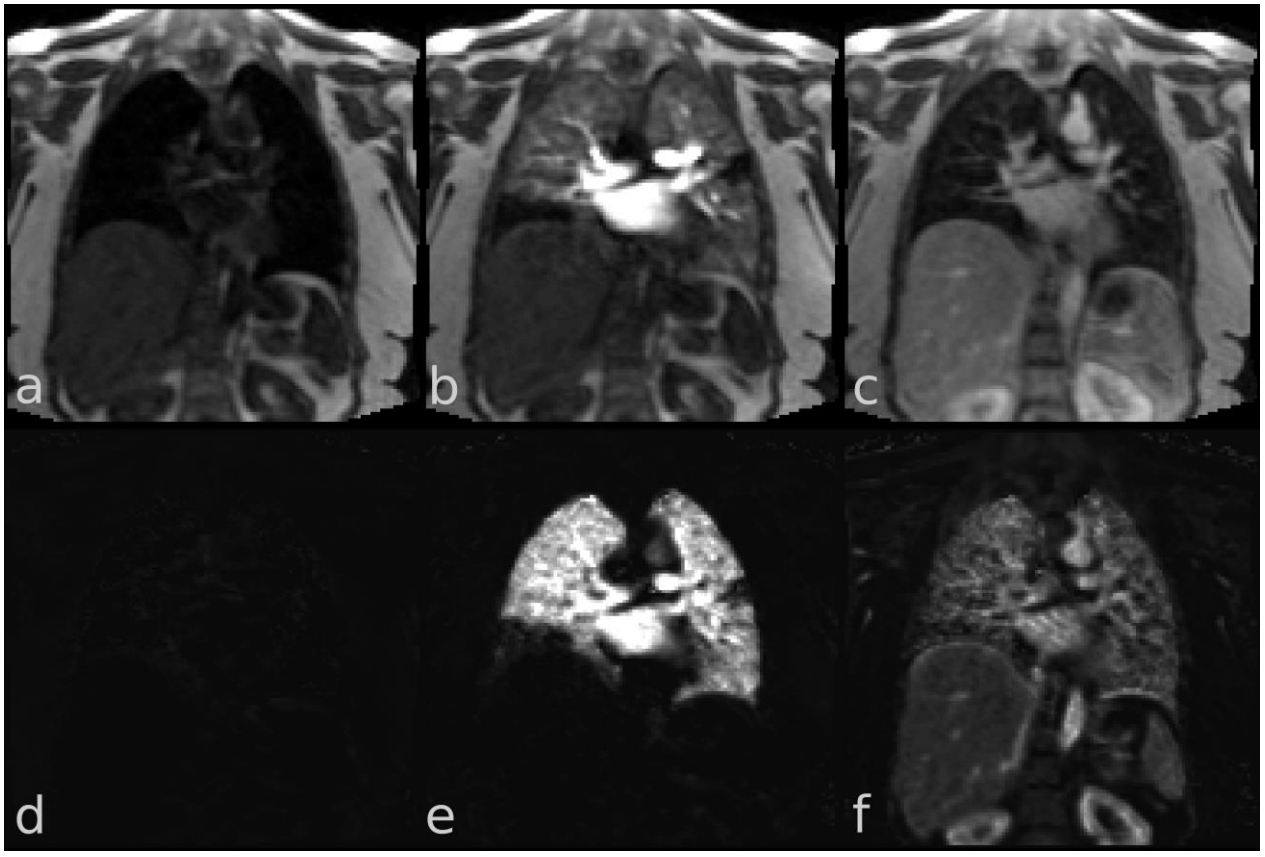

Figure 1: DCE MRI data of a patient with acute pulmonary embolism (subject #2). Top row: unprocessed data before contrast agent arrival (a), at peak pulmonary intensity (b) and in a late phase (c). Bottom row (d-f): Relative enhancement at the same time points. Time frames 1, 9 and 70 were used.

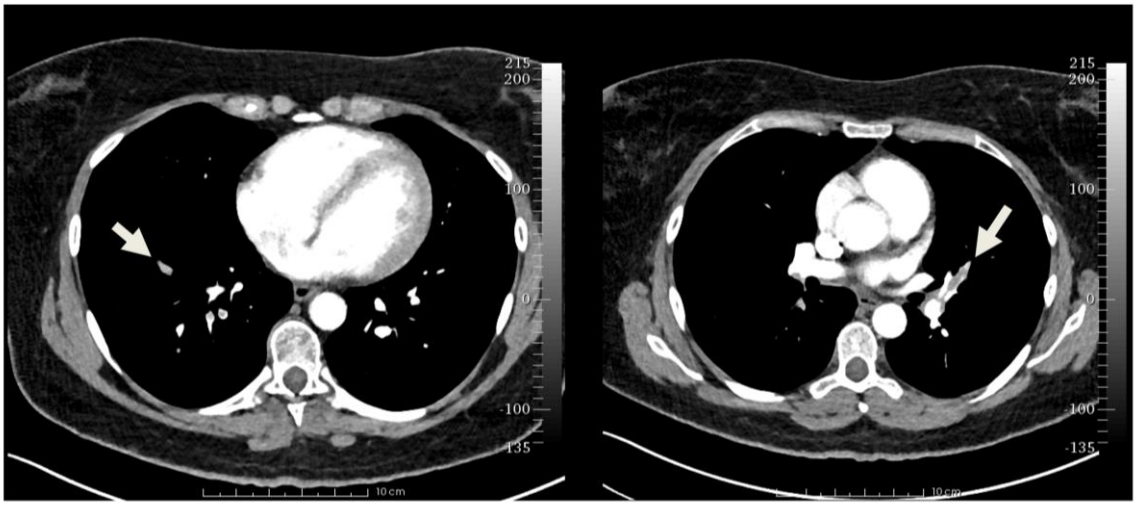

Figure 2: Axial CTPA images of the same patient as in Fig. 1. The thrombi that correspond to the perfusion defects visible in Fig. 1 are indicated with arrows.

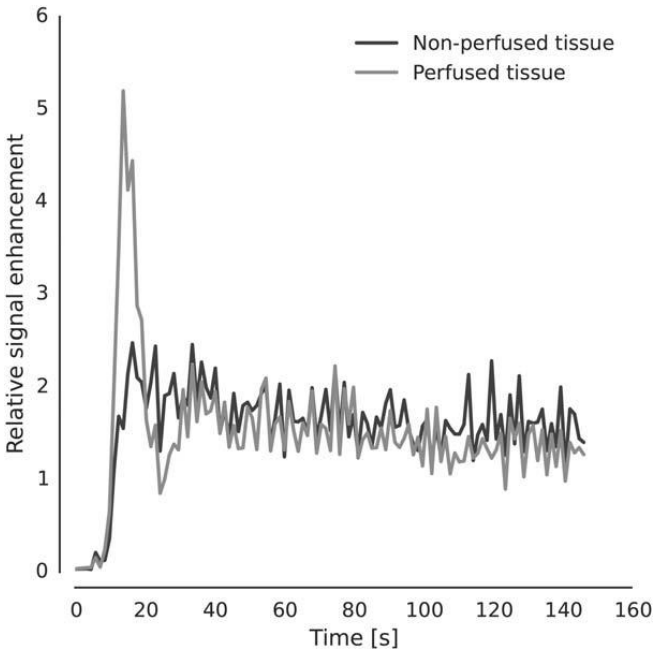

Figure 3: Time courses of the relative signal enhancement in the small perfusion defect from Fig. 1 and in a region with equal size in unaffected pulmonary parenchyma on the contralateral side. Strong differences both in the signal and in the signal enhancement occur during the bolus passage, whereas the differences before contrast agent administration and in the late phase of the acquisition are much smaller.

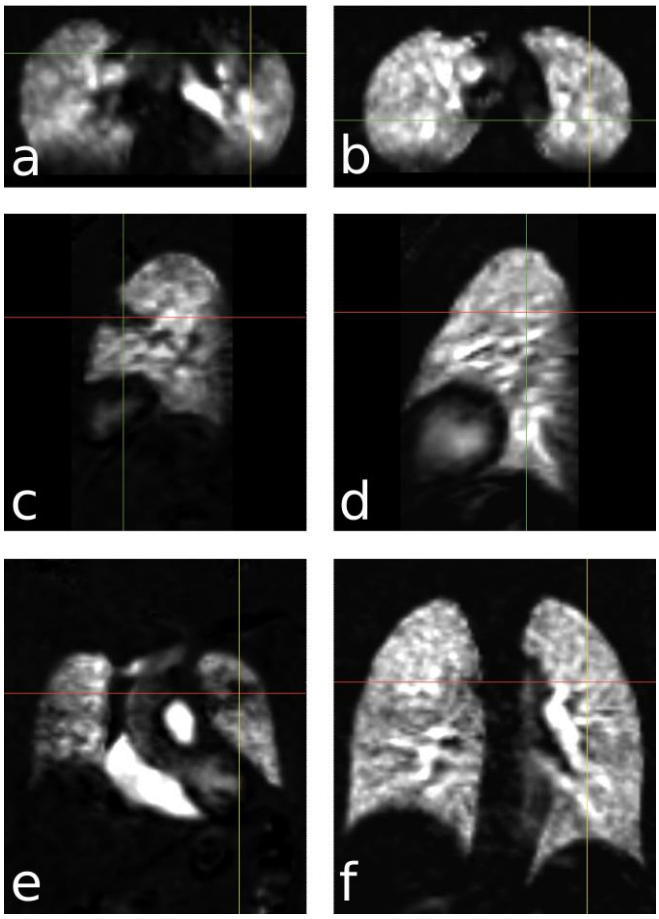

Figure 4: Maps of relative signal enhancement in subject #10 (patient, left column, a,c,e) and subject #8 (healthy volunteer, right column,b,d,f). Displayed are axial, sagittal and coronal cross-sections at the positions indicated by the crosshair. In the patient data, a perfusion defect in the left lung can be appreciated at the crosshair position, most notably in the sagittal cross-section.

Table 3: Findings in all patients and volunteers[a]

Subject ID	Status	Laterality	CT	MR1	MR2
2	patient	left	1	1	1
2	patient	right	1	1	1
3	patient	left	0	1	0
3	patient	right	1	1	1
6	patient	left	1	0	0
6	patient	right	1	1	1
7	patient	left	1	1	1
7	patient	right	1	1	1
10	patient	left	1	1	1
10	patient	right	1	1	1
14	patient	left	1	1	1
14	patient	right	1	1	1
15	patient	left	1	1	0
15	patient	right	1	1	1
17	patient	left	1	1	1
17	patient	right	1	1	1
1	volunteer	left	0	0	0
1	volunteer	right	0	0	0
4	volunteer	left	0	0	0
4	volunteer	right	0	0	0
5	volunteer	left	0	0	0
5	volunteer	right	0	0	0
8	volunteer	left	0	0	0
8	volunteer	right	0	0	0
9	volunteer	left	0	0	0
9	volunteer	right	0	0	0
11	volunteer	left	0	0	0
11	volunteer	right	0	0	0
12	volunteer	left	0	0	0
12	volunteer	right	0	0	0
13	volunteer	left	0	0	0
13	volunteer	right	0	0	0
16	volunteer	left	0	0	1
16	volunteer	right	0	0	1
18	volunteer	left	0	0	0
18	volunteer	right	0	0	0

[a] '1' indicates the presence of pulmonary embolism in the respective lung

Table 4: Statistical results with 95% confidence intervals.

	Reader 1	Reader 2
Sensitivity	0.93 (0.68, 1.00)	0.87 (0.60, 0.98)
Specificity	0.95 (0.76, 1.00)	0.90 (0.70, 0.99)
Positive predictive value	0.93 (0.68, 1.00)	0.87 (0.60, 0.98)
Negative predictive value	0.95 (0.76, 1.00)	0.90 (0.70, 0.99)

The value of the 3D acquisition is demonstrated in axial, coronal and sagittal cross sections of patient and volunteer data in Fig. 4: The perfusion defect in the patient is most notable in the sagittal cross-section.

The findings in all patients and volunteers are summarized in Table 3: In 15 of the 16 patients' lungs, perfusion defects were observed in DCE MRI. In the volunteers, reader 1 observed no perfusion defects in all 20 volunteer lungs, whereas reader 2 described a small perfusion defect in subject #16.

We found a substantial inter-reader agreement of $\kappa = 0.72$ (95% confidence interval, 0.38-1.0). The sensitivity of free-breathing DCE MRI for the detection of PE was 93% and 87% for reader 1 and reader 2, respectively, with a specificity of 95% and 90%, respectively. All statistical results including positive and negative predictive values of both readers are reported in Table 4.

Fisher's exact t-test revealed strong agreement ($p < 0.001$) between DCE MRI and CTPA findings.

Discussion

In this study, we were able to demonstrate that DCE MRI, acquired during free breathing, allows for reliable detection of acute pulmonary embolism. To visualize the pulmonary perfusion and to suppress background signal, we calculated the signal enhancement relative to the pre-contrast signal and evaluated the data at the time point of maximal pulmonary enhancement. This signal enhancement is heavily perfusion-weighted and can thus be used to discriminate parenchyma that is affected by pulmonary embolism from unaffected parenchyma with high sensitivity.

This strategy was inspired by dual-energy computed tomography (DECT), where a map of the iodine concentration is calculated after administration of iodine-based contrast agent(10, 11, 23). A DECT-acquisition is limited to a single or only few time frames , so that the timing of the acquisition is important (12), since the maximal contrast between normal and affected lung tissue occurs at the time of peak pulmonary enhancement. Compared to DECT, the timing of the DCE acquisition is much less critical, since images can be acquired continuously. In DCE MRI, the time frame with maximal

pulmonary enhancement can easily be selected retrospectively.

With free-breathing DCE MRI, we were able to detect perfusion defects caused by pulmonary embolism in very good agreement with contrast-enhanced CTPA, which is regarded as the gold standard for the diagnosis of pulmonary embolism (2). Of the 16 patient lungs, 15 were affected by pulmonary embolism, as demonstrated by CTPA. In patient #6, both readers did not locate a perfusion defect in the left lung, however, in CTPA, an obstruction was detected. The reason for this discrepancy may be the temporal separation of CT and MRI scans of 3 days. During that time, the patient received therapy, which may have resulted in a reperfusion of the affected parenchyma. It can also be speculated that the thrombus detected in CTPA may have had no hemodynamic relevance.

An explanation for the DCE MRI findings with no correlation in CT (patient #3, left lung) may be either that new occlusions occurred in the time between CTPA and MRI, or that the observed perfusion defects are not related to obstructions in the pulmonary arteries. This is also supported by the finding of a perfusion defect in an otherwise healthy volunteer (subject #16, only reader 2).

Usually, pulmonary perfusion measurements are performed during breath hold to minimize the effects of breathing motion. MR perfusion imaging has been used for the detection of PE in several studies (24, 25) with promising results, albeit with acquisitions during breath-hold. Recent studies demonstrated, however, that imaging and quantification of pulmonary perfusion with DCE MRI is also feasible when performed during free breathing (18) and can even lead to more reproducible results (19). Patients with pulmonary embolism are unlikely to sustain a breath hold for extended time. Additionally, it is not unlikely that patients breathe in strongly after extended breath hold, which may cause strong motion artefacts. Consequently, free breathing acquisitions do not only increase patient compliance and patient comfort, but are also beneficial for data quality. In the context of our study, breathing-related motion could cause artefacts within each acquired volume as well as in the in the derived maps of relative signal enhancement. We did not observe significant motion artifacts in the unprocessed acquired volumes. This may be due to the k-space sampling scheme that was employed in our acquisition sequence: the TWIST sequence samples large parts of the peripheral k-space in a random fashion, which is more robust with respect to motion than conventional, linear sampling schemes. In the calculated maps of relative signal enhancement, subtraction-related artifacts can occur e.g. close to the diaphragm, in particular, when images are subtracted that were acquired during different phases of the breathing cycle. However, we did not find subtraction-related artefacts that limited the diagnosis of perfusion defects.

Several other studies have used MRI for the evaluation of pulmonary embolism. The largest report of these is the PIOPED III study (26), which reported a sensitivity for the detection of pulmonary embolism of 78% using MR pulmonary angiography, which is used for the direct detection of blood clots and requires careful timing of acquisition and injection. Similar values were reported in a study by Kalb et al. (27) for a 3D gradient echo sequence used for an acquisition after bolus passage and during breath-hold. In contrast to these studies, our protocol required no timing of acquisition or injection and no breath-hold, while achieving higher sensitivity and comparable specificity. Moreover, it can be expected that sensitivity can be increased even more, when the free-breathing DCE MRI evaluation is combined with pulmonary MR angiography for direct thrombus detection. This has been demonstrated in a previous study (24), where the highest diagnostic accuracy was reached when DCE MRI was combined with high-resolution contrast-enhanced MR angiography.

Here, we have demonstrated that free-breathing DCE MRI is useful for the assessment of perfusion defects in acute PE. However, free-breathing DCE MRI, potentially combined with quantification of pulmonary perfusion, may also be useful in a range of other pulmonary diseases where focal or global perfusion defects can occur such as pulmonary hypertension (28), pulmonary emphysema, or chronic obstructive pulmonary disease (29).

Our study has three main limitations. First, the MR and CT examinations were separated between one and five days, and during that time, the patients received therapy, which may have negative impact on the agreement between CTPA and DCE MRI. Nevertheless, the agreement is still excellent. Second, we included only a small number of patients, which is the main reason for the comparatively

large confidence intervals. Therefore, the sensitivity and specificity that we observed warrant further studies in larger patient groups. Third, no patients without PE were available for this study. In order to be able to assess the specificity of free-breathing DCE MRI, we therefore included a group of healthy volunteers with no history or symptoms of pulmonary embolism; for this group, no CTPA was available.

Our results are only preliminary, we believe that the acquisition during free breathing, the absence of exposure to ionizing radiation and the minimal amount of post-processing that is required makes this method attractive for clinical application, especially in younger patients. Our results warrant a study of diagnostic accuracy of free-breathing DCE MRI in a larger patient group, in which also patients with negative CTPA should be included. It should be noted that the total acquisition time in further studies could be shortened considerably, since contrast between perfused and non-perfused regions is maximal at the time point of the first bolus passage during the lung.

In conclusion, we were able to demonstrate that DCE MRI, acquired during free breathing, is a promising technique for the assessment of PE with high sensitivity and specificity which does not require patient cooperation in terms of breath-holding and does not expose the patient to ionizing radiation.

References

1. Konstantinides S, Goldhaber SZ: Pulmonary embolism: risk assessment and management. *Eur Heart J* 2012; 33:3014–3022.

2. Zhang LJ, Lu GM, Meinel FG, McQuiston AD, Ravenel JG, Schoepf UJ: Computed tomography of acute pulmonary embolism: state-of-the-art. *Eur Radiol* 2015.

3. Schoepf UJ, Costello P: CT angiography for diagnosis of pulmonary embolism: state of the art. *Radiology* 2004; 230:329–337.

4. Stein PD, Fowler SE, Goodman LR, et al.: Multidetector computed tomography for acute pulmonary embolism. *N Engl J Med* 2006; 354:2317–2327.

5. Wittram C, Maher MM, Yoo AJ, Kalra MK, Shepard J-AO, McLoud TC: CT Angiography of Pulmonary Embolism: Diagnostic Criteria and Causes of Misdiagnosis1. *RadioGraphics* 2004; 24:1219–1238.

6. Meinel FG, Nance JW, Schoepf UJ, et al.: Predictive Value of Computed Tomography in Acute Pulmonary Embolism: Systematic Review and Meta-Analysis. *Am J Med* 2015.

7. Moody AR, Liddicoat A, Krarup K: Magnetic resonance pulmonary angiography and direct imaging of embolus for the detection of pulmonary emboli. *Invest Radiol* 1997; 32:431–440.

8. van Beek EJR, Wild JM, Fink C, Moody AR, Kauczor H-U, Oudkerk M: MRI for the diagnosis of pulmonary embolism. *J Magn Reson Imaging* 2003; 18:627–640.

9. Biederer J, Mirsadraee S, Beer M, et al.: MRI of the lung (3/3)—current applications and future perspectives. *Insights Imaging* 2012; 3:373–386.

10. Thieme SF, Becker CR, Hacker M, Nikolaou K, Reiser MF, Johnson TRC: Dual energy CT for the assessment of lung perfusion—Correlation to scintigraphy. *Eur J Radiol* 2008; 68:369–374.

11. Nikolaou K, Thieme S, Sommer W, Johnson T, Reiser MF: Diagnosing pulmonary embolism: new computed tomography applications. *J Thorac Imaging* 2010; 25:151–160.

12. Meinel FG, Graef A, Sommer WH, Thierfelder KM, Reiser MF, Johnson TRC: Influence of vascular enhancement, age and gender on pulmonary perfused blood volume quantified by dual-energy-CTPA. *Eur J Radiol* 2013; 82:1565–1570.

13. Dournes G, Verdier D, Montaudon M, et al.: Dual-energy CT perfusion and angiography in chronic thromboembolic pulmonary hypertension: diagnostic accuracy and concordance with radionuclide scintigraphy. *Eur Radiol* 2014; 24:42–51.

14. Schönfeld C, Cebotari S, Voskrebenzev A, et al.: Performance of perfusion-weighted Fourier decomposition MRI for detection of chronic pulmonary emboli: Detection of Chronic PE. *J Magn Reson Imaging* 2015; 42:72–79.

15. Ohno Y, Higashino T, Takenaka D, et al.: MR angiography with sensitivity encoding (SENSE) for suspected pulmonary embolism: comparison with MDCT and ventilation–perfusion scintigraphy. *Am J Roentgenol* 2004; 183:91–98.

16. Nikolaou K, Schoenberg SO, Brix G, et al.: Quantification of Pulmonary Blood Flow and Volume in Healthy Volunteers by Dynamic Contrast-Enhanced Magnetic Resonance Imaging Using a Parallel Imaging Technique: *Invest Radiol* 2004; 39:537–545.

17. Ingrisch M, Dietrich O, Attenberger UI, et al.: Quantitative pulmonary perfusion magnetic resonance imaging: influence of temporal resolution and signal-to-noise ratio. *Invest Radiol* 2010; 45:7–14.

18. Maxien D, Ingrisch M, Meinel FG, Reiser M, Dietrich O, Nikolaou K: Quantification of pulmonary perfusion with free-breathing dynamic contrast-enhanced MRI--a pilot study in healthy volunteers. *RöFo Fortschritte Auf Dem Geb Röntgenstrahlen Nukl* 2013; 185:1175–1181.

19. Ingrisch M, Maxien D, Schwab F, Reiser MF, Nikolaou K, Dietrich O: Assessment of pulmonary perfusion with breath-hold and free-breathing dynamic contrast-enhanced magnetic resonance imaging: quantification and reproducibility. *Invest Radiol* 2014; 49:382–389.

20. Ingrisch M, Sourbron S: Tracer-kinetic modeling of dynamic contrast-enhanced MRI and CT: a primer. *J Pharmacokinet Pharmacodyn* 2013; 40:281–300.

21. Fedorov A, Beichel R, Kalpathy-Cramer J, et al.: 3D Slicer as an image computing platform for the Quantitative Imaging Network. *Magn Reson Imaging* 2012; 30:1323–1341. [*Quantitative Imaging in Cancer*]

22. R Core Team: *R: A Language and Environment for Statistical Computing*. Vienna, Austria: R Foundation for Statistical Computing; 2014.

23. Meinel FG, Graef A, Bamberg F, et al.: Effectiveness of automated quantification of pulmonary perfused blood volume using dual-energy CTPA for the severity assessment of acute pulmonary embolism. *Invest Radiol* 2013; 48:563–569.

24. Kluge A, Luboldt W, Bachmann G: Acute Pulmonary Embolism to the Subsegmental Level: Diagnostic Accuracy of Three MRI Techniques Compared with 16-MDCT. *Am J Roentgenol* 2006; 187:W7–W14.

25. Kluge A, Gerriets T, Stolz E, et al.: Pulmonary perfusion in acute pulmonary embolism: agreement of MRI and SPECT for lobar, segmental and subsegmental perfusion defects. *Acta Radiol* 2006; 47:933–940.

26. Stein PD, Chenevert TL, Fowler SE, et al.: Gadolinium-Enhanced Magnetic Resonance Angiography for Pulmonary Embolism. *Ann Intern Med* 2010; 152:434–W143.

27. Kalb B, Sharma P, Tigges S, et al.: MR imaging of pulmonary embolism: diagnostic accuracy of contrast-enhanced 3D MR pulmonary angiography, contrast-enhanced low-flip angle 3D GRE, and nonenhanced free-induction FISP sequences. *Radiology* 2012; 263:271–278.

28. Nikolaou K, Schoenberg SO, Attenberger U, et al.: Pulmonary arterial hypertension: diagnosis with fast perfusion MR imaging and high-spatial-resolution MR angiography--preliminary experience. *Radiology* 2005; 236:694–703.

29. Molinari F, Fink C, Risse F, Tuengerthal S, Bonomo L, Kauczor H-U: Assessment of differential pulmonary blood flow using perfusion magnetic resonance imaging: comparison with radionuclide perfusion scintigraphy. *Invest Radiol* 2006; 41:624–630.